

NANOMECHANICS OF PROTEIN FILAMENTS

BY SAMUEL J. BALDWIN, ANDREW S. QUIGLEY, AND LAURENT KREPLAK

One of the hallmarks of mammalian tissues is the presence of several interconnected filamentous protein networks both within each cell, the so-called cytoskeleton [1], and within the extracellular matrix [2]. Each network is a dynamic assembly of protein filaments and associated molecules that can sustain mechanical stresses as well as be remodeled in response to the same. Considering the importance of filamentous networks in maintaining the structural integrity of tissues, it comes as no surprise that their mechanical properties have attracted a lot of attention both experimentally and theoretically [3,4]. At the network level, most studies so far ignore all the molecular level diversity found in protein filaments and treat them as slender rods with a combination of entropic and enthalpic elasticity [5]. This simple approach has been very successful in identifying common features in the mechanical properties of a wide range of networks built of actin filaments, intermediate filaments, fibrin fibers and collagen fibrils, for example. It does not mean however that these different networks are interchangeable; in fact each type of protein filament has evolved to achieve a defined set of physical and biological functions. This is why measuring the mechanical properties of single protein filaments is also of great interest even if it is to some extent more challenging than dealing with macroscopic networks.

Any method developed to test the mechanical properties of single protein filaments has to contend with three issues: the filaments are small with diameters between 1 and 100s of nanometers, the forces necessary to bend or stretch them are anywhere in the pico-Newton to micro-Newton range, and the measurements have to be repeated many times to be representative of a large population. Currently there are many approaches available from micropipette manipulation [6] to optical tweezers [7], microelectromechanical systems (MEMS) [8], stretchable substrates [9], and atomic force microscopy (AFM) [10].

SUMMARY

We discuss atomic force microscopy based approaches to study the structural and mechanical properties of protein filaments using intermediate filaments and collagen fibrils as examples.

As an example we will discuss a group of AFM-based approaches that have proven successful in testing cytoskeletal filaments and collagen fibrils.

The AFM has three main modes of operations: imaging, force spectroscopy or indentation, and manipulation (Fig. 1a) [11]. Each of these can provide useful mechanical information on single filaments attached to a solid support in a liquid environment.

NANOMECHANICS OF CYTOSKELETAL FILAMENTS

The mammalian cell's cytoskeleton is composed of three types of protein filaments: actin filaments, intermediate filaments such as keratin, vimentin and lamin, and microtubules [1]. For each of these filaments, the three main mechanical quantities of interest are the degree of bending due to thermal fluctuations, the Young's and shear moduli, and their ultimate tensile properties, typically their maximum extensibility and their ultimate tensile strength.

Imaging flexible filaments on a surface

In first approximation cytoskeletal protein filaments are not different from long, flexible, polymer chains. Single protein filaments in solution at constant temperature experience shape fluctuations that can be characterized using the worm-like chain model by a persistence length P [12]. In turn, P provides an estimate of the bending rigidity of the filament assuming it is a uniform, homogenous, elastic material [12]. For cytoskeletal filaments the shape fluctuations occur over sub-micrometer to millimeter length scales depending on the protein and can be measured by fluorescence microscopy [13]. Another approach is to let the filaments attach to a flat substrate and image their "frozen" contour by AFM [12]. For this method to work the filaments must be dilute enough on the substrate to avoid any overlap with neighbors, they must appear flexible on the scale of their contour length and they must have reached their equilibrium conformation on the substrate. The last point is typically difficult to assess and requires testing different buffer conditions or substrates with different surface chemistry. In the case of cytoskeletal filaments it is often not feasible to change buffer conditions because they have a strong impact on the assembly state of the filaments. For example divalent cations like calcium or



Samuel J. Baldwin
<Samuel.Baldwin@dal.ca >

Andrew S. Quigley
<Andrew.Quigley@dal.ca >

and

Laurent Kreplak
<Kreplak@dal.ca >

Dalhousie University,
Department of Physics and Atmospheric Science,
POBOX 15000,
Halifax, NS B3L 1C5

magnesium tend to bundle actin [14] and intermediate filaments [15]. Varying buffer and substrates for three different types of intermediate filaments demonstrated a wide range of morphologies from twisted bundles to beaded filaments and thin tapes [16]. For vimentin intermediate filaments in standard assembly conditions, we investigated mica, graphite and glass, and obtained a persistence length of 1 micrometer [12]. Assuming these filaments are uniform homogeneous elastic cylinders with a diameter of 10 nm, we get an equivalent Young's modulus of 8 MPa. This number describes the flexibility of vimentin filaments that are much longer than their persistence length, 1 micrometer. What happens if we test these filaments on a length scale smaller than their persistence length?

Bending intermediate filaments

The most direct way to measure the bending stiffness of a beam is a two-point or three-point bending test. For microtubules that have a persistence length in the millimeter range, the two types of tests were performed using optical tracking [17] and AFM imaging [18], respectively. With the optical method, it was possible to demonstrate that bending of microtubules is in fact length dependent [17]. With AFM imaging of microtubules absorbed on a membrane with manufactured slits of varying width around 100 nm, it was possible to estimate the Young's and shear moduli using elasticity theory [18]. In principle if the microtubules were just cylinders filled with an isotropic material, the ratio of Young's modulus to shear modulus is typically smaller than 3, however the experimentally measured ratio is around 1000 indicating that microtubules are anisotropic.

For vimentin intermediate filaments we used a similar AFM approach using porous alumina membranes with a pore size of 250 nm [19]. The apparent bending modulus in this geometry was 300 MPa, which puts a lower bound on the filaments Young's modulus assuming no shear deformation [19]. There is then a contradiction between the persistence length measurements discussed above and this three point bending result. One way to resolve it is to consider the possibility of shear deformations within the vimentin intermediate filaments. Interestingly, vimentin intermediate filaments are built by the lateral packing of staggered double stranded alpha-helical coiled-coils which are slender 45 nm long rods with a diameter around 2 nm [20]. The Young's modulus of a single coiled-coil is in the order of 1 GPa [21]. Assuming this is also the Young's modulus of a vimentin intermediate filament, the three-point bending test yields a shear modulus of 2.5 MPa. As expected the vimentin intermediate filament is strongly anisotropic and the Young's modulus estimated from the persistence length data appear to be on the order of the shear modulus. In other words thermal fluctuations of the filament's shape are mostly due to a shear deformation mode at the molecular level.

Stretching intermediate filaments

So far we have only discussed the mechanical properties of intermediate filaments in the small deformation limit. To access the tensile properties of these filaments, one can take advantage of the manipulation capabilities of the AFM. Intermediate filaments are absorbed on a flat substrate in liquid and the AFM probe, pressed against the surface, is moved on a path perpendicular to the filament's axis (Fig. 1a) [1]. For the right AFM cantilever stiffness, one observes that the filament is locally bent and stretched by the probe until it breaks. AFM imaging after manipulation reveals that 100 to 500 nm long segments of the filaments were extended by 50 to 250% strain and that the diameter of the filaments decreased from 10-12 nm down to 2 nm for the largest strains (Fig. 1b) [22]. Considering that the maximum extensibility of an alpha-helical coiled-coil is around 150% strain [23], these results confirm that two molecular mechanisms are at play during elongation, unfolding of the coiled coils and sliding of these units past each other. Furthermore, the AFM offers the possibility to measure the force applied to the filament during manipulation. Forces to break a single intermediate filament are between 1 and 5 nN [24,25]. The force-displacement data can also be fit using a two-state model in order to extract the unfolding force of a single coiled-coil unit, which is around 10 pN for desmin intermediate filaments [26].

NANOMECHANICS OF COLLAGEN FIBRILS

Collagen fibrils are another ubiquitous protein filament within the mammalian kingdom. These fibrils have diameters between 50 and 500 nm. They form densely packed networks in skin, tendons, ligaments, cartilage and bone and act as a mechanical scaffold for cells within these tissues. Similarly to intermediate filaments, collagen fibrils are linear aggregates of staggered rod-shaped collagen molecules 300 nm long and 1.5 nm in diameter [27]. However collagen fibrils also have specific-covalent crosslinks between molecules that further stabilize the axial staggering pattern and that are essential for the fibrils load bearing functions within tissues [28]. At the single fibril level, two main AFM derived approaches are commonly used to assess mechanical properties: nanoindentation and tensile testing.

Probing collagen fibrils' molecular architecture via nanoscale indentation

To perform a nanoindentation experiment, the AFM probe is pressed into a single collagen fibril until a target deflection of the cantilever is achieved. Knowing the tip-sample geometry, one can fit the force-displacement curve and extract the indentation modulus, which is around 1-5 MPa [10] for a hydrated fibril or 1-5 GPa [29] for a dried fibril at low indentation speeds. Due to the geometry of the nanoindentation experiment and the anisotropic nature of the collagen fibrils, the indentation modulus is not an intrinsic mechanical constant such as the Young's modulus; rather it measures the degree of lateral cohesion between collagen molecules within the fibril.

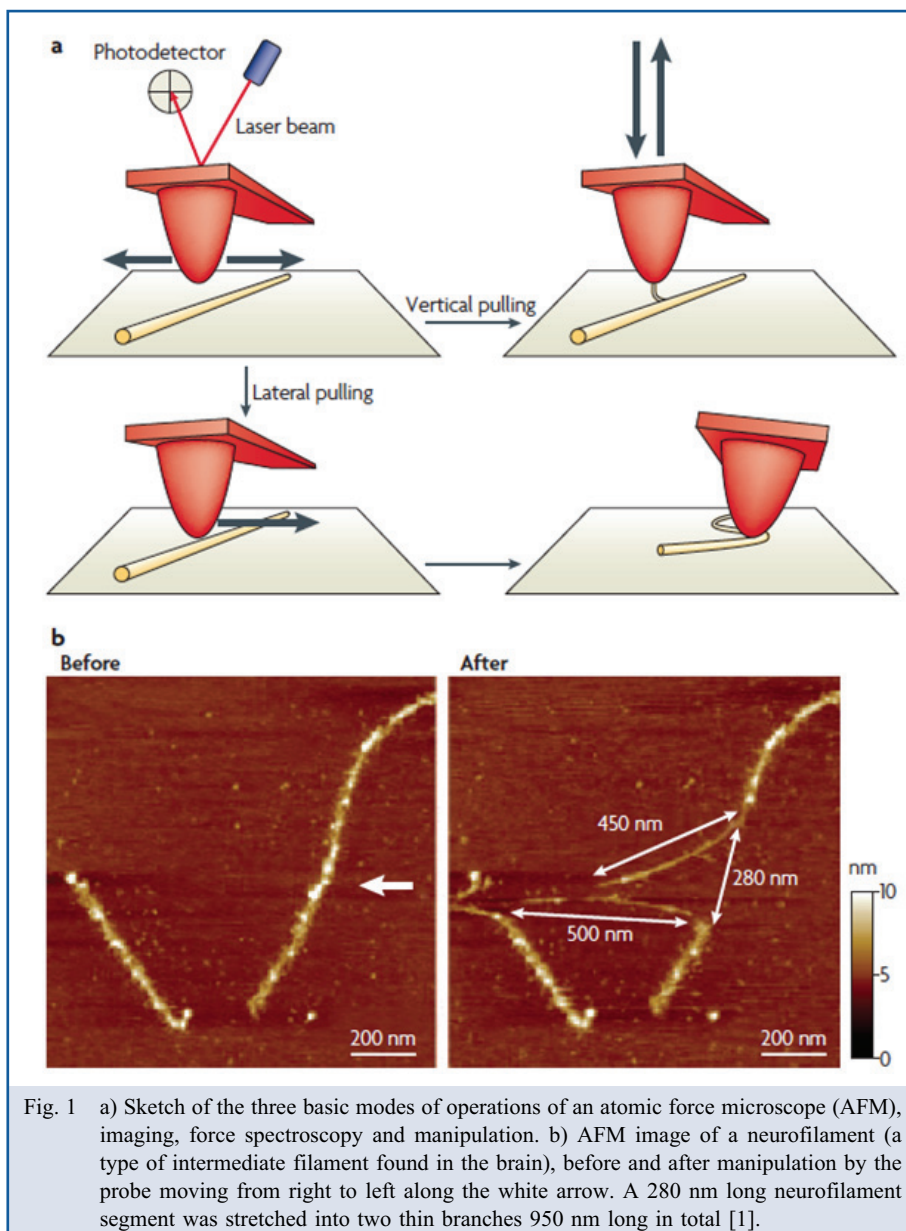


Fig. 1 a) Sketch of the three basic modes of operations of an atomic force microscope (AFM), imaging, force spectroscopy and manipulation. b) AFM image of a neurofilament (a type of intermediate filament found in the brain), before and after manipulation by the probe moving from right to left along the white arrow. A 280 nm long neurofilament segment was stretched into two thin branches 950 nm long in total [1].

As such the indentation modulus should be sensitive to the density and connectivity of crosslinks, and to the density of collagen molecules in the fibril cross-section. Interestingly the axial stagger of the molecules within the fibril is expected to generate regular gaps between the molecules that produce a periodic fluctuation in molecular density with a characteristic length scale of 67 nm [30]. The gap regions of the fibrils are expected to have 4/5 the molecular density of the overlap regions, and this provides a density contrast over a length scale that can be easily resolved using a sharp AFM probe. However, nano-indentation measurements along single dried collagen fibril revealed a factor of two in indentation modulus between gap and overlap regions [29]. Similar measurements were carried along hydrated collagen fibrils in various buffer

conditions but revealed no contrast in indentation modulus between gap and overlap regions [10]. In order to understand the lack of contrast along hydrated collagen fibrils we explored the impact of the tip velocity on the indentation modulus. We observed that for tip velocities between 0.1 and 100 $\mu\text{m/s}$, the indentation modulus of a collagen fibril in water is proportional to the logarithm of the velocity [27] as expected for rubbers above the glass transition temperature [31]. Above 100 $\mu\text{m/s}$ the indentation modulus increased by a factor of 3 to 5 over one decade [27]. This sharp increase in indentation modulus is also observed for rubbers below the glass transition temperature and is the signature of a characteristic relaxation time of the tip-fibril interaction. As long as the indentation occurs over a time scale longer than the relaxation time, viscous effects dominate and the indentation modulus is insensitive to contrasts in molecular density. When the indentation occurs over a time scale shorter than the relaxation time, viscous modes of deformation are “frozen out”, the fibril appears stiffer than before and one expects the indentation modulus to be sensitive to how densely packed the molecules are in the vicinity of the probe. This assumption was confirmed by performing nanoindentation maps along single collagen fibrils in water with a tip velocity of 600 $\mu\text{m/s}$. We observed that the indentation modulus of the gap regions was 80% of the one measured in the overlap regions, confirming the molecular density prediction (Fig. 2a and c) [27].

These experiments served as a proof of principle to study the effect of plastic deformation, generated by mechanical overload, on the fibrils structure. We were then able to demonstrate that fibrils extracted from overloaded bovine tail tendons have a core with preserved molecular packing surrounded by a loose and disordered shell (Fig. 2b and d) [32]. In order to establish the relationship between stress, strain and structural damage, we need to move away from tensile testing of full tendons where loading is not homogeneous to tensile experiments at the single fibril level.

Tensile testing of single collagen fibrils

So far there has been two ways of measuring the stress-strain curve of a single collagen fibril: using an AFM in the force

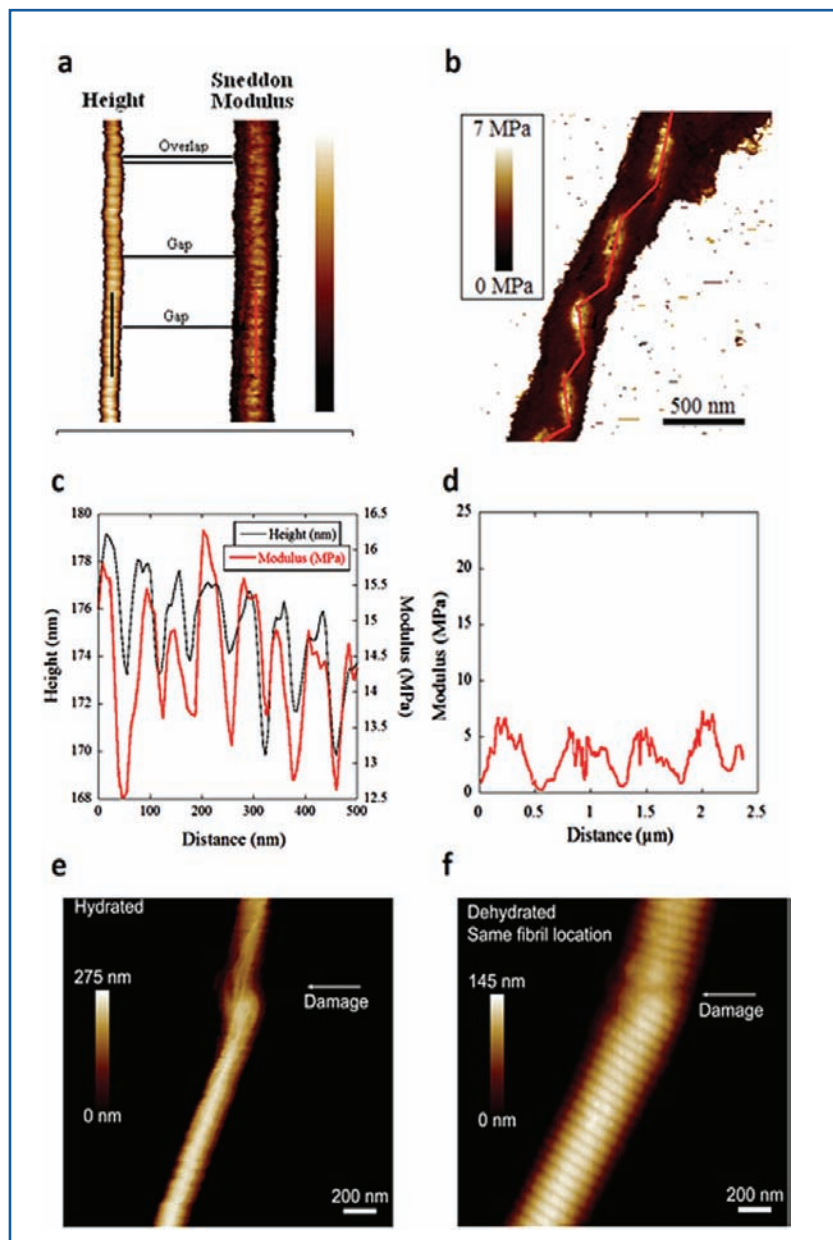


Fig. 2 a) Matched height and indentation modulus data obtained for a hydrated collagen fibril extracted from rat tail, the bar represents $2\ \mu\text{m}$ (adapted from [27]). b) Indentation modulus map of a hydrated collagen fibril extracted from a cyclically overloaded bovine tail tendon (adapted from [32]). c) Matched height and indentation modulus profiles taken along the apex of the fibril in a). Note that the periodic gap and overlap fluctuations in height, the overlap being always higher than the gap, are matched with similar fluctuations in modulus (adapted from [27]). d) Indentation modulus profile taken along the apex of the overloaded fibril in b) (adapted from [32]). Notice the periodic gap and overlap fluctuation in c) compared to the micrometer scale fluctuation in d). The decrease in indentation modulus from c) to d) is due to the presence of a disordered shell surrounding a more compact core. e) and f) hydrated and dehydrated images of the same fibril after tensile failure (adapted from [33]). Notice the striking difference of morphology at the damaged site.

spectroscopy mode [34] and using microelectromechanical systems (MEMS) [8]. A collagen fibril typically breaks between 20 and 50% strain depending on its length and pulling speed. The force necessary to reach failure is in the 1-10 μN range. Fibrils broken using these two approaches show either no damage except at the ruptured ends or lateral molecular packing disruption similar to the core-shell morphology described above. For both methods, it is not easy to study the effect of loading without rupture on the fibril structure. To circumvent this issue, we have developed an in-plane stretching technique inspired from previous nanomanipulation studies on intermediate filaments (Fig. 1b) [33]. Fibrils are dried on a substrate to allow laying down thin strips of glue at regular intervals. This procedure generates isolated fibril segments that can be rehydrated and manipulated by moving an AFM probe perpendicular to the segment's long axis, stretching the fibril like a bowstring. The entire manipulation process can be recorded with a video microscope as long as the fibrils have a diameter above 100 nm, which is the case for most fibrils extracted from mature tendons. After loading, the fibrils remain on the substrate and can be imaged in air or in liquid (Fig. 2e and f). Using this approach we observed that the indentation modulus of fibrils stretched to 3-4% and released dropped by a factor of 2, while the hydrated height of the fibrils increased by 30% [33]. Subsequent stretching of the same pre-conditioned fibrils to strains up to 20% without rupture yielded a decrease in indentation modulus by a up to a factor of 5 while the height of the fibrils randomly increased by 10 to 70% without a clear strain dependence [33]. Furthermore, some of the fibrils ruptured during the pulling process, which gave us an opportunity to observe the vast morphological differences between the hydrated and dehydrated state of a damaged fibril (Fig. 2e and f) [33]. In the future we intend to also record the force necessary to pull the fibrils and correlate the observed changes in fibril architecture with stress-strain data.

CONCLUSION

It is clear from the few examples highlighted here that we are only beginning to understand the complexity arising from the self-assembly of proteins into filaments. Measuring mechanical properties at the single filament level is a

promising way forward in this field, as it will allow researchers to dissect the impact of small changes at the protein level on the properties of the filamentous assembly. However it should

also be complemented by structural measurements at the single filament level through, for example, nanoscale vibrational spectroscopy techniques [35,36].

REFERENCES

1. H. Herrmann, H. Bar, L. Kreplak, S.V. Strelkov, and U. Aebi, "Intermediate filaments: from cell architecture to nanomechanics", *Nat Rev. Mol. Cell Biol.*, **8**, 562-573 (2007).
2. C. Frantz, K.M. Stewart, and V.M. Weaver, "The extracellular matrix at a glance", *J. Cell. Sci.*, **123**, 4195-4200 (2010).
3. L. Deng, X. Trepap, J.P. Butler, E. Millet, K.G. Morgan, D.A. Weitz, and J.J. Fredberg, "Fast and slow dynamics of the cytoskeleton", *Nat. Mater.*, **5**, 636-640 (2006).
4. A.J. Licup, S. Munster, A. Sharma, M. Sheinman, L.M. Jawerth, B. Fabry, D.A. Weitz, and F.C. MacKintosh, "Stress controls the mechanics of collagen networks", *Proc. Natl. Acad. Sci. U S A*, **112**, 9573-9578 (2015).
5. C. Storm, J.J. Pastore, F.C. MacKintosh, T.C. Lubensky, and P.A. Janmey, "Nonlinear elasticity in biological gels", *Nature*, **435**, 191-194 (2005).
6. Y. Tsuda, H. Yasutake, A. Ishijima, and T. Yanagida, "Torsional rigidity of single actin filaments and actin-actin bond breaking force under torsion measured directly by in vitro micromanipulation", *Proc. Natl. Acad. Sci. U S A*, **93**, 12937-12942 (1996).
7. F. Kilchherr, C. Wachauf, B. Pelz, M. Rief, M. Zacharias, and H. Dietz, "Single-molecule dissection of stacking forces in DNA", *Science*, **353**, 5508 (2016).
8. Z.L. Shen, M.R. Dodge, H. Kahn, R. Ballarini, and S.J. Eppell, "In vitro fracture testing of submicron diameter collagen fibril specimens", *Biophys. J.*, **99**, 1986-1995 (2010).
9. D. Fudge, D. Russell, D. Beriault, W. Moore, E.B. Lane, and A.W. Vogl, "The intermediate filament network in cultured human keratinocytes is remarkably extensible and resilient", *PLoS One*, **3**, e2327 (2008).
10. C.A. Grant, D.J. Brockwell, S.E. Radford, and N.H. Thomson, "Tuning the elastic modulus of hydrated collagen fibrils", *Biophys. J.*, **97**, 2985-2992 (2009).
11. L. Kreplak, "Introduction to Atomic Force Microscopy (AFM) in Biology", *Curr. Protoc. Protein. Sci.*, **85**, 17 7 1-17 7 21 (2016).
12. N. Mucke, L. Kreplak, R. Kirmse, T. Wedig, H. Herrmann, U. Aebi, and J. Langowski, "Assessing the flexibility of intermediate filaments by atomic force microscopy", *J. Mol. Biol.*, **335**, 1241-1250 (2004).
13. C.P. Brangwynne, G.H. Koenderink, E. Barry, Z. Dogic, F.C. MacKintosh, and D.A. Weitz, "Bending dynamics of fluctuating biopolymers probed by automated high-resolution filament tracking", *Biophys. J.*, **93**, 346-359 (2007).
14. T. Maier and T. Haraszti, "Reversibility and Viscoelastic Properties of Micropillar Supported and Oriented Magnesium Bundled F-Actin", *PLoS One*, **10**, e0136432 (2015).
15. C. Dammann and S. Koster, "Dynamics of counterion-induced attraction between vimentin filaments followed in microfluidic drops", *Lab Chip*, **14**, 2681-2687 (2014).
16. N. Mucke, R. Kirmse, T. Wedig, J.F. Leterrier, and L. Kreplak, "Investigation of the morphology of intermediate filaments adsorbed to different solid supports", *J. Struct. Biol.*, **150**, 268-276 (2005).
17. F. Pampaloni, G. Lattanzi, A. Jonas, T. Surrey, E. Frey, and E.L. Florin, "Thermal fluctuations of grafted microtubules provide evidence of a length-dependent persistence length", *Proc. Natl. Acad. Sci. U S A*, **103**, 10248-10253 (2006).
18. A. Kis, S. Kasas, B. Babic, A.J. Kulik, W. Benoit, G.A. Briggs, C. Schonenberger, S. Catsicas, and L. Forro, "Nanomechanics of microtubules", *Phys. Rev. Lett.*, **89**, 248101 (2002).
19. C. Guzman, S. Jeney, L. Kreplak, S. Kasas, A.J. Kulik, U. Aebi, and L. Forro, "Exploring the mechanical properties of single vimentin intermediate filaments by atomic force microscopy", *J. Mol. Biol.*, **360**, 623-630 (2006).
20. A.A. Chernyatina, D. Guzenko, and S.V. Strelkov, "Intermediate filament structure: the bottom-up approach", *Curr. Opin. Cell Biol.*, **32**, 65-72 (2015).
21. C.W. Wolgemuth and S.X. Sun, "Elasticity of alpha-helical coiled coils", *Phys. Rev. Lett.*, **97**, 248101 (2006).
22. L. Kreplak, H. Bar, J.F. Leterrier, H. Herrmann, and U. Aebi, "Exploring the mechanical behavior of single intermediate filaments", *J. Mol. Biol.*, **354**, 569-577 (2005).
23. I. Schwaiger, C. Sattler, D.R. Hostetter, and M. Rief, "The myosin coiled-coil is a truly elastic protein structure", *Nat. Mater.*, **1**, 232-235 (2002).
24. L. Kreplak and H. Bar, "Severe myopathy mutations modify the nanomechanics of desmin intermediate filaments", *J. Mol. Biol.*, **385**, 1043-1051 (2009).
25. L. Kreplak, H. Herrmann, and U. Aebi, "Tensile properties of single desmin intermediate filaments", *Biophys. J.*, **94**, 2790-2799 (2008).
26. D.B. Staple, M. Loparic, H.J. Kreuzer, and L. Kreplak, "Stretching, unfolding, and deforming protein filaments adsorbed at solid-liquid interfaces using the tip of an atomic-force microscope", *Phys. Rev. Lett.*, **102**, 128302 (2009).
27. S.J. Baldwin, A.S. Quigley, C. Clegg, and L. Kreplak, "Nanomechanical mapping of hydrated rat tail tendon collagen I fibrils", *Biophys. J.*, **107**, 1794-1801 (2014).

28. S.P. Robins, "Analysis of the crosslinking components in collagen and elastin", *Methods Biochem. Anal.*, **28**, 329-379 (1982).
29. M. Minary-Jolandan and M.F. Yu, "Nanomechanical heterogeneity in the gap and overlap regions of type I collagen fibrils with implications for bone heterogeneity", *Biomacromolecules*, **10**, 2565-2570 (2009).
30. A.J. Hodge and F.O. Schmitt, "The Charge Profile of the Tropocollagen Macromolecule and the Packing Arrangement in Native-Type Collagen Fibrils", *Proc. Natl. Acad. Sci. U S A*, **46**, 186-197 (1960).
31. D. Tranchida, Z. Kiflie, S. Acierno, and S. Piccarolo, "Nanoscale mechanical characterization of polymers by atomic force microscopy (AFM) nanoindentations: viscoelastic characterization of a model material", *Measurement Science and Technology*, **20**, 095702-095710 (2009).
32. S.J. Baldwin, L. Kreplak, and J.M. Lee, "Characterization via atomic force microscopy of discrete plasticity in collagen fibrils from mechanically overloaded tendons: Nano-scale structural changes mimic rope failure", *J. Mech. Behav. Biomed. Mater.*, **60**, 356-366 (2016).
33. A.S. Quigley, S.P. Veres, and L. Kreplak, "Bowstring Stretching and Quantitative Imaging of Single Collagen Fibrils via Atomic Force Microscopy", *PLoS One*, **11**, e0161951 (2016).
34. R.B. Svensson, H. Mulder, V. Kovanen, and S.P. Magnusson, "Fracture mechanics of collagen fibrils: influence of natural cross-links", *Biophys. J.*, **104**, 2476-2484 (2013).
35. C. Gullekson, L. Lucas, K. Hewitt, and L. Kreplak, "Surface-sensitive Raman spectroscopy of collagen I fibrils", *Biophys. J.*, **100**, 1837-1845 (2011).
36. R. Wiens, C.R. Findlay, S.G. Baldwin, L. Kreplak, J.M. Lee, S.P. Veres, and K.M. Gough, "High spatial resolution (1.1 μm and 20 nm) FTIR polarization contrast imaging reveals pre-rupture disorder in damaged tendon", *Faraday Discuss*, **187**, 555-573 (2016).